Journal of Rajasthan Academy of Physical Sciences
ISSN: 0972-6306; URL: http://raops.org.in
Vol.22, No.1&2, January-June, 2023, 114-123

MHD STAGNATION POINT FLOW OF WILLIAMSON FLUID THROUGH POROUS MEDIA OVER A STRETCHING SURFACE UNDER THE INFLUENCE OF THERMAL RADIATION AND VISCOUS DISSIPATION

Hina Yadav[1] and Mamta Goyal[2]
[1,2]Department of Mathematics, University of Rajasthan, Jaipur-302004, India
Email: [1]hinarao297@gmail.com, [2]mamtagoyal1245@gmail.com

Abstract: MHD stagnation point flow of Williamson fluid through porous media over a stretching surface under influence of thermal radiation and viscous dissipation is examined. Along a set of proper similarity transformation governing PDE's are converted to non- linear ODEs after that solved numerically by Runge-Kutta (RK4) scheme allied with shooting technique. Via tables and graphs numerical outcomes for local Nusselt number and skin friction coefficient, also temperature and velocity field are interpreted. Ascendancy of Prandtl number, Radiation parameter, non-Newtonian Williamson fluid parameter, Eckert number, Magnetic parameter, velocity and thermal slip parameter properties are discussed. Present outcomes compared with existing results and observed excellent validation.

Keywords: MHD, Williamson fluid, porous media, Thermal radiation, Viscous dissipation.

MSC Classification: 76W05, 76D05, 76Sxx, 78A40.

1. Introduction

During last decades, enormous efforts have been implemented in fluid flow on account of stretching sheet operation to find out valuable elucidation of manufacturing and industrial processes, like polymer preparing, paper making, food perpetuating processes, crystal manufacturing, and filtration in petroleum industries. On this topic for the beneficial and debt importance, several researchers interested to examine about the recent findings which work for this field. Sakiadis [15] first contributed on fluid flow owing to stretched surface. Williamson [16] studied flow of pseudo-plastic objects and displayed model to explain, behavior of pseudo-plastic material and describe beneficial consequence of plastic flows, and identified that viscous flow is certainly diverse from plastic flows. Krishnamurthy et al. [8] analyzed time independent flow of Williamson fluid considering nanoparticle on account of linearly stretching surface considering effect of chemical reaction and melting heat transfer. Nadeem et al. [13,14] have studied Williamson fluid flow in account of stretching surface. By Manjula et al. [10] MHD Williamson nanofluid flow through porous medium with viscous dissipation was investigated. Mahapatra and Gupta [11] have studied time independent two-dimensional incompressible viscous fluid flow towards stagnation point over flat deformable sheet. Megahed [12] have studied boundary layer flow of Williamson fluid and heat transfer account to nonlinearly stretching surface, also considering viscous dissipation and thermal radiation circumstance. Malik [9] solved numerical problem of MHD flow of Williamson fluid over stretching cylinder. Khan and Khan [7] analyze steady boundary layer flow of Williamson fluid. Aman et al. [1] analyzed time independent stagnation-point flow of viscous and incompressible fluid past linearly stretching/shrinking surface in account of magnetic field. Bouslimi et al. [4] studied Williamson nanofluid in presence of electromagnetic force and thermal radiation on stretching sheet via porous medium with presence of heat generation/absorption and Joule heating, also considering effect of Brownian motion and thermophoresis coefficients. Bhattacharyya [2,3] have studied effect of slip factors on heat transfer and boundary layer stagnation point flow past a shrinking surface. Chaudhary et al. [5,6] analyzed MHD stagnation point flow over stretching sheet. Sakiadis [15] studied boundary layer behaviour on continuous moving solid surfaces and Williamson [16] studied the flow of pseudoplastic.

2. Mathematical Formulation

We presume slip effects on time independent two-dimensional stagnation point flow of Williamson fluid towards a stretching surface as demonstrated in Figure 1. Here external velocity is $u_e(x) = ax$ and stretching velocity is $u_w(x) = cx$, where a and c are constants and governing equations are:

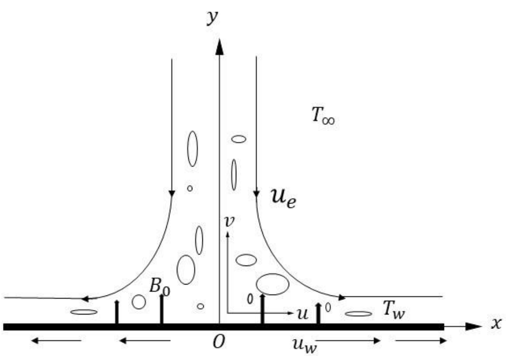

Figure 1: Sketch of physical model

$$\frac{\partial u}{\partial x} + \frac{\partial v}{\partial y} = 0, \tag{1}$$

$$u\frac{\partial u}{\partial x} + v\frac{\partial u}{\partial y} = u_e\frac{du_e}{dx} + v\frac{\partial^2 u}{\partial y^2} + \sqrt{2}v\Gamma\frac{\partial u}{\partial y}\frac{\partial^2 u}{\partial y^2} - \frac{\sigma B_0^2}{\rho}u - \frac{v}{k_p^*}u, \tag{2}$$

$$u\frac{\partial T}{\partial x} + v\frac{\partial T}{\partial y} = \frac{\kappa}{\rho C_p}\frac{\partial^2 T}{\partial y^2} + \frac{\mu}{\partial C_p}\left(1 + \frac{\Gamma}{\sqrt{2}}\frac{\partial u}{\partial y}\right)\left(\frac{\partial u}{\partial y}\right)^2 - \frac{1}{\rho C_p}\frac{\partial q_r}{\partial y}. \tag{3}$$

With boundary conditions:

$$u = u_w + \gamma_1 \mu \frac{\partial u}{\partial y}, \quad v = 0, \quad T = T_w + \beta_1 \frac{\partial T}{\partial y} \quad at \quad y = 0, \tag{4}$$

$$u \to u_{e,} \quad T \to T_\infty \quad as \quad y \to \infty. \tag{5}$$

Where, in x and y directions corresponding velocity is u and v. Wall temperature is $T_w(x) = T_\infty + bx^2$, ν is kinematic viscosity, applied magnetic field is B_0, k_p^* is permeability of porous media, Temperature of fluid is T, q_r is radiative flux, κ represent thermal conductivity, γ_1 is velocity slip parameter, β_1 is thermal slip parameter, ρ represent fluid density, specific heat represented by C_p , Γ represent time constant and viscosity is μ.

For radiation we have used Roseland's approximation and obtain $q_r = -\left(\frac{4}{3}\frac{\sigma^*}{\kappa_1}\right)\frac{\partial T^4}{\partial y}$, where σ^* represents Stefan-Boltzmann constant, κ_1 represent mean absorption factor. About free stream temperature by using Taylor series, we have

$$T^4 = 4TT_\infty^3 - 3T_\infty^4. \tag{6}$$

Now Equation (3) transform into

$$u\frac{\partial T}{\partial x} + v\frac{\partial T}{\partial y} = \frac{\kappa}{\rho C_p}\frac{\partial^2 T}{\partial y^2} + \frac{\mu}{\rho C_p}\left(1 + \frac{\Gamma}{\sqrt{2}}\frac{\partial u}{\partial y}\right)\left(\frac{\partial u}{\partial y}\right)^2 + \frac{16\sigma^* T_\infty^3}{3\kappa_1 \rho C_p}\frac{\partial^2 T}{\partial y^2}. \tag{7}$$

3. Problem Solution

Now, we propose similarity variables as following:

$$\eta = (c/\nu)^{1/2} y, \psi = \sqrt{c\nu} f(\eta), \theta(\eta) = \frac{T - T_\infty}{T_w - T_\infty}, \tag{8}$$

where Ψ denote stream function

$$u = \frac{\partial \psi}{\partial y}, \; v = -\frac{\partial \psi}{\partial x}, \tag{9}$$

By using equation (8), equation (1) satisfies identically and equations (2) and (7), becomes

$$f''' + ff'' - (M + K_p)f' - f'^2 + \lambda f'' f''' + \epsilon^2 = 0, \tag{10}$$

$$(1 + R)\theta'' - Pr\left[(2\theta f' - f\theta') - Ecf''^2 - \frac{1}{2}Ec\lambda f''^3\right]. \tag{11}$$

Where $Pr = \frac{\nu \rho C_p}{\kappa}$ is Prandtl number, $Ec = \frac{c^2}{C_p b}$ is Eckert number, $\lambda = x\Gamma\sqrt{\frac{2c^3}{\nu}}$ is non-Newtonian Williamson parameter and $\epsilon = \frac{a}{c}$ is stretching parameter. The boundary conditions (4) and (5) turn into

$$f(0) = 0, \; f'(0) = 1 + \gamma f''(0), \; \theta(0) = 1 + \beta\theta'(0), \tag{12}$$

$$f'(\eta) \to \epsilon, \theta(\eta) \to 0 \; as \; \eta \to \infty. \tag{13}$$

Where, dimensionless velocity parameter is $\gamma = \gamma^* \rho (c\nu)^{1/2}$ and thermal slip parameter is $\beta = \beta^* \left(\frac{c}{\nu}\right)^{1/2}$. If wall temperature continues constant then β = 0. Skin friction coefficient C_f and local Nusselt number Nu are accorded as

$$C_f = \frac{\tau_w}{\rho u_w^2}, \tag{14}$$

$$Nu = \frac{-x}{T_w - T_\infty}\left(\frac{\partial T}{\partial y}\right)_{y=0}. \tag{15}$$

The surface shear stress τ_w is given by

$$\tau_w = \mu \frac{\partial u}{\partial y}\left[1 + \Gamma \sqrt{\frac{1}{2}\frac{\partial u}{\partial y}}\right], \tag{16}$$

Using similarity variables give

$$C_f Re_x^{1/2} = f''(0) + \frac{\lambda}{2}(f''(0))^2, \tag{17}$$

$$Nu_x Re_x^{-1/2} = -\theta'(0). \tag{18}$$

where $Re_x = \frac{cx^2}{\nu}$ is local Reynolds number.

4. Numerical Solution

We encounter numerical solution of problem by using *RK4* method allied with shooting technique. MATLAB computer programming is utilized for calculations. Appropriate estimates of $\boldsymbol{f''}$ and $\boldsymbol{\theta'}$ as $\boldsymbol{\eta = 0}$ are taken with shooting technique to attain boundary conditions at $\boldsymbol{\eta} \to \infty$ which are ϵ and 1. We assume $\Delta\boldsymbol{\eta} = \mathbf{0.01}$ and value for $\boldsymbol{\eta_{max} = 6}$. Equations (10) and (11) with boundary conditions (12)-(13) are modified into system of differential equations of order one as following:

$$f_1' = f_2 \tag{19}$$

$$f_2' = f_3 \tag{20}$$

$$f_3' = \frac{1}{1+\lambda f_3}\left[f_2^2 + \left(M + K_p\right) f_2 - f_1 f_3 - \epsilon^2\right] \tag{21}$$

$$f_4' = f_5 \tag{22}$$

$$f_5' = \frac{Pr}{1+R}\left[(2\theta f' - f\theta') - Ec\left(1 + \frac{1}{2}\lambda f''^2\right) f''\right] \tag{23}$$

5. Discussion of the Results

In Table 1 validation of present results is established by comparing with results of Mahapatra and Gupta [11].

Table 1: Comparison for variations in values of *ϵ* when *Pr* = 1, *λ* = 0, *M* = 0, K_p = 0, *γ* = 0, *β* = 0, *R* = 0 and *Ec* = 0.

ϵ	Mahapatra and Gupta [7] $f''(0)$	Present $f''(0)$
0.1	-0.9694	-0.96943
0.2	-0.9181	-0.91811
0.5	-0.6673	-0.667261
2	2.0175	2.017502
3	4.7293	4.729282

Table 2 represents numerical values of local Nusselt number and local skin friction parameter for various parameters and default values of parameters for calculation are taken ϵ=3, M=0.1, Kp=0.1, Pr=1, R=1, β=1, γ=1, λ=1 and Ec=1.

Fig.2 and Fig. 3 depicts increment in values of Williamson parameter deflates velocity and inflate temperature profile, because ratio of relaxation time to retardation time is Williamson parameter, so when we increase λ, relaxation time will increase as a consequence of this, viscosity of fluid increases. Increased viscosity results deflation in velocity and inflation in temperature. Fig.4 demonstrate impact of Magnetic parameter on temperature profile. Increasing values of M inflate temperature due to the retarding Lorenz force. Fig.5 shows the effect of Permeability parameter on velocity profile. Velocity deflates with increasing values of Kp, because Kp in inversely proportional to permeability of porous media. Fig.6 and Fig.7 elucidate impact of velocity slip parameter γ on velocity and temperature profile. γ inflates velocity and deflate temperature profile. Fig.8 shows impact of temperature slip factor β on temperature. Temperature slip appear when sheet temperature and temperature of fluid flow are not in thermal equilibrium. Temperature of the fluid decrease with increasing temperature slip parameter. Fig.9 demonstrate radiation parameter effect on temperature. Inflation in R reduce Rosseland radiation absorptivity κ, radiative heat flux inflate as κ deflate i.e. radiative heat transfer rate to fluid will increase so, fluid temperature inflate. Fig.10 demonstrate impact of Prandtl number on temperature profile. Inflation in Pr, temperature decreases because of Prandtl number is proportional to the specific heat i.e. more the heat requires to increase temperature for a given amount. Fig.11 demonstrate that for increment in Eckert number, temperature profile inflates because an increment in values of Ec, self-heating in fluid increase, so temperature inflate. Fig.12 demonstrate increment in values of stretching parameter ϵ increases velocity profile because of stretch, which reduce viscous effect on flow so, momentum boundary layer thickness is reduced along increment in ϵ hence increased velocity. Fig.13 depicts effect of ϵ on temperature. Temperature reduces when ϵ is increased.

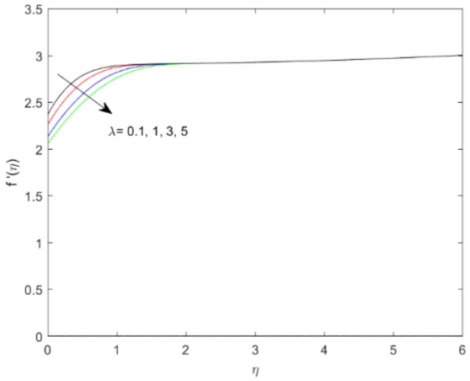

Figure 2: Distribution of velocity for variations in λ

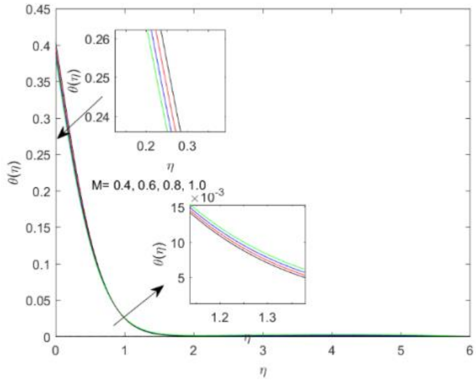

Figure 4: Distribution of temperature for variations in M

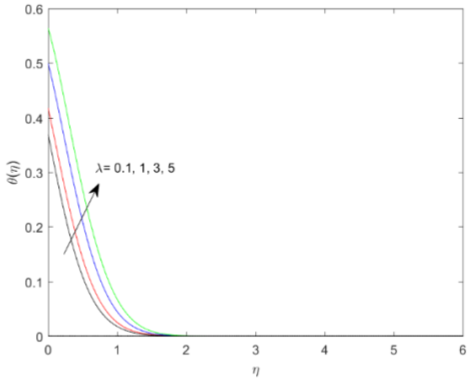

Figure 3: Distribution of temperature for variations in λ

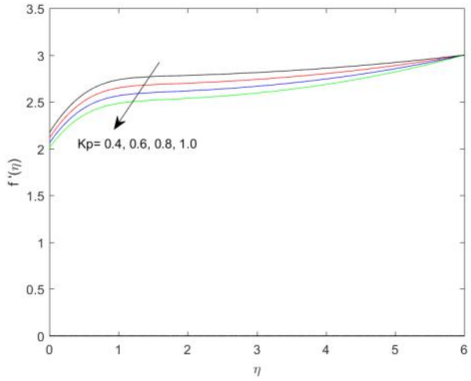

Figure 5: Distribution of velocity for variations in K_p

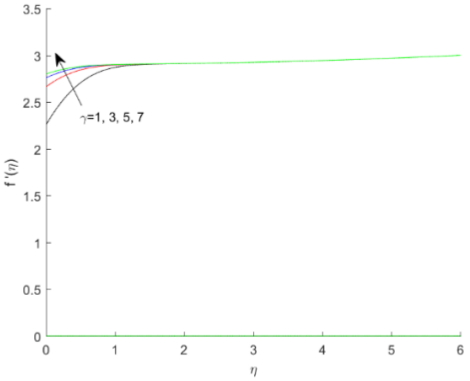

Figure 6: Distribution of velocity for variations in γ

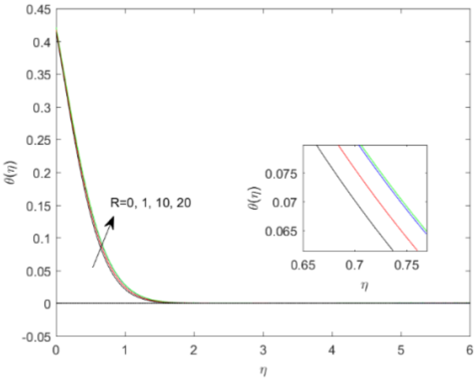

Figure 9: Distribution of temperature for variations in R

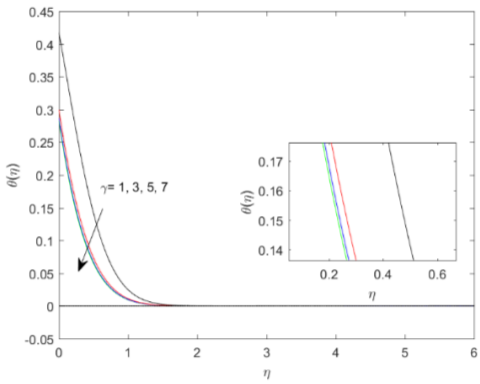

Figure 7: Distribution of temperature for variations in γ

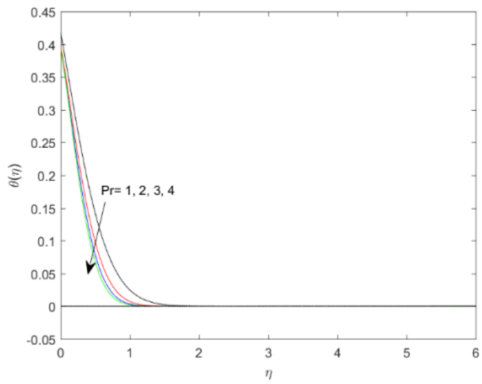

Figure 10: Distribution of temperature for variations in P

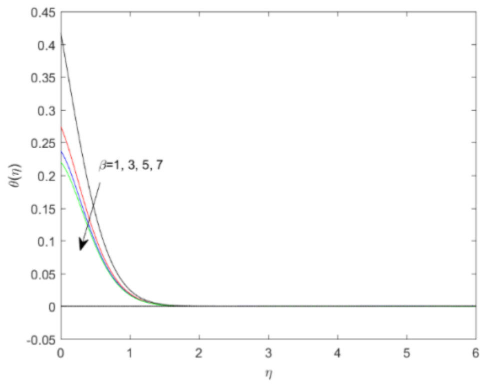

Figure 8: Distribution of temperature for variations in β

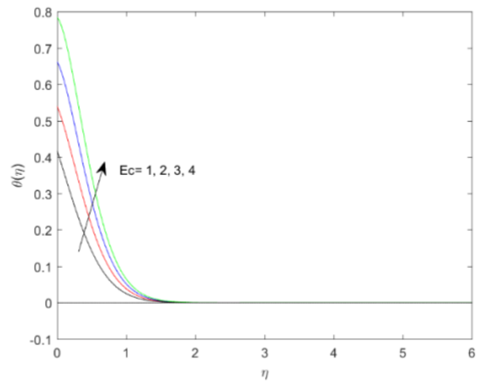

Figure 11: Distribution of temperature for variations in Ec

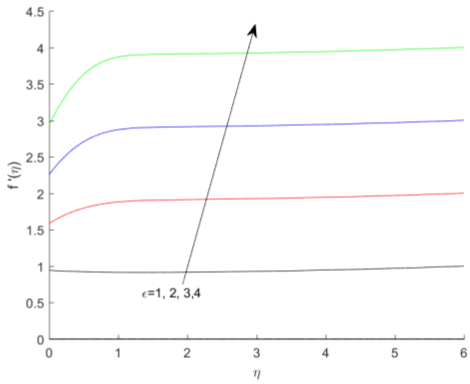

Figure 12: Distribution of velocity for variations in ϵ

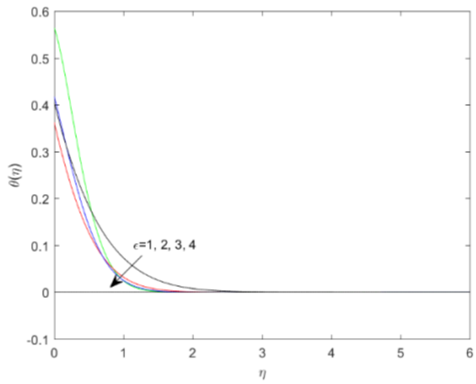

Figure 13: Distribution of temperature for variations in ϵ

Table 2: For variations in values of λ, M, K_p, γ, β, R, Pr and Ec, Values of $f''(0)$ and $\theta'(0)$.

λ	M	K_p	γ	β	R	Pr	Ec	ϵ	$f''(0)$	$\theta'(0)$
0.1									1.365443	-0.63102
1									1.258559	-0.582993
3									1.129589	-0.500858
5									1.052466	-0.436155
	0.4								1.171616	-0.596724
	0.6								1.115900	-0.604585
	0.8								1.061971	-0.611491
	1.0								1.009816	-0.617508
		0.4							1.171616	-0.596724
		0.6							1.115900	-0.604585
		0.8							1.061971	-0.611491
		1.0							1.009816	-0.617508
			1						1.258559	-0.582993
			3						0.554638	-0.700710
			5						0.351911	-0.713310
			7						0.257274	-0.717084
				1					1.258559	-0.582993
				3					1.258559	-0.241874
				5					1.258559	-0.152590
					0				1.258559	-0.586372
					1				1.258559	-0.582993
					10				1.258559	-0.579768
					20				1.258559	-0.579395
						1			1.258559	-0.582993
						2			1.258559	-0.603430
						3			1.258559	-0.607829
						4			1.258559	-0.607906
							1		1.258559	-0.582993
							3		1.258559	-0.241874
							5		1.258559	-0.152590
							7		1.258559	-0.111451
								1	-0.057540	-0.595260
								2	0.586529	-0.638413
								3	1.258559	-0.582993
								4	1.939496	-0.43644

6. Conclusions

In this paper a theoretical analysis of MHD stagnation point flow of Williamson fluid over a stretching surface implanted in porous medium under influence of thermal radiation and viscous dissipation have been done. We have acquired following results:

(i) Increment in Williamson and Permeability parameter deflate velocity profile and inflate temperature profile.

(ii) Thermal boundary layer decrease for increment in values of thermal slip parameter.

(iii) Temperature profile inflates as radiation parameter and Eckert number increases.

(iv) Temperature profile deflate for increasing Prandtl number.

(v) For increasing stretching parameter skin friction coefficient increases.

Acknowledgement: Author (Hina Yadav) is gratefully acknowledged the University grants Commission of India, for financial abutment (Ref.No.: 1181/(CSIR-UGC NET DEC 2018)) under scheme of Junior Research Fellowship and Referee for valuable comments and suggestions.

References

[1] Aman, F., Ishak, A. and Pop, I. (2013). Magnetohydrodynamic stagnation-point flow towards a stretching/shrinking sheet with slip effects. International Communications in Heat and Mass Transfer **47**, 68–72. https://doi.org/ 10.1016/j.icheatmasstransfer. 2013.06.005

[2] Bhattacharyya, K., Mukhopadhyay, S. and Layek, G. C. (2011). Slip effects on boundary layer stagnation-point flow and heat transfer towards a shrinking sheet. International Journal of Heat and Mass Transfer **54**(1-3), 308–313. https://doi.org/10. 1016/j.ijheatmasstransfer.2010.09.041

[3] Bhattacharyya, K., Mukhopadhyay, S. and Layek, G. C. (2011). MHD boundary layer slip flow and heat transfer over a flat plate. Chinese Physics Letters **28**(2), 0247011- 0247014. DOI10.1088/0256-307X/28/2/024701

[4] Bouslimi, J., Omri, M., Mohamed, R.A., Mahmoud, K.H., Abo-Dahab, S.M. and Soliman, M.S. (2021). MHD Williamson Nanofluid Flow over a Stretching Sheet through a Porous Medium under Effects of Joule Heating, Nonlinear Thermal Radiation, Heat Generation/Absorption, and Chemical Reaction. Advances in Mathematical Physics, Hindawi, 1-16. https://doi.org/10.1155/2021/9950993

[5] Chaudhary, S., Singh, S. and Chaudhary, S. (2016). Numerical solution for magnetohydrodynamic stagnation point flow towards a stretching or shrinking surface in a saturated porous medium. Int. J. Pure Appl. Math. **106**, 141-155. doi:10.12732/ijpam.v106i1.11

[6] Chaudhary, S. and Choudhary, M.K. (2018). Partial slip and thermal radiation effects on hydro-magnetic flow over an exponentially stretching surface with suction or blowing. Thermal Science **22**(2), 797-808 https://doi.org/10.2298/TSCI160127150C

[7] Khan, Najeeb and Khan, H.A. (2014). A Boundary layer flows of non-Newtonian Williamson fluid. Nonlinear Eng. **3**, 107-115. https://doi.org/10.1515/nleng-2014-0002

[8] Krishnamurthy, M.R., Prasannakumara, B.C., Gireesha, B.J. and Gorla, R.S.R. (2016). Effect of chemical reaction on MHD boundary layer flow and melting heat transfer of Williamson nanofluid in porous medium. Eng. Sci. and Tech., an Int. J. **19**(1), 53-61. https://doi.org/10.1016/j.jestch.2015.06.010

[9] Malik, M.Y. and Salahuddin, T. (2015). Numerical solution of MHD stagnation point flow of Williamson fluid model over a stretching cylinder. Int. J. Nonlin. Sci. Num. **16**, 161-164. https://doi.org/10.1515/ijnsns-2014-0035

[10] Manjula, N., Govardhan, K. and Rajashekar, M.N. (2019). Effect of Viscous Dissipation on MHD Williamson Nanofluid Flow in a Porous Medium, International Journal of Recent Technology and Engineering **8**(3), 5795-5802. DOI:10.35940/ijrte. C4861.098319

[11] Mahapatra, T.R. and Gupta, A.S. (2002). Heat transfer in stagnation-point flow towards a stretching sheet, Heat and Mass transfer **38**(6), 517-521. http://dx.doi.org/ 10.1007/s002310100215

[12] Megahed, A.M. (2019). Williamson fluid flow due to a nonlinearly stretching sheet with vic- sous dissipation and thermal radiation, Journal of the Egyptian Mathematical Society **27**(12), 1-10. https://doi.org/10.1186/s42787-019-0016-y

[13] Nadeem, S. and Hussain, S.T. (2014). Heat transfer analysis of Williamson fluid over exponentially stretching surface. Appl. Math. Mech. Engl. **35**(4), 489–502. https://doi.org/ 10.1007/s10483-014-1807-6

[14] Nadeem, S., Hussain, S.T. and Lee, C. (2013). Flow of a Williamson fluid over a stretching sheet. Brazilian J. of Chem. Eng. **30**(3), 619-625. https://doi.org/ 10.1590/S0104-66322013000300019

[15] Sakiadis, B.C. (1961). Boundary layer behavior on continuous moving solid surfaces. I. Boundary layer equations for two-dimensional and axisymmetric flow. II. Boundary layer on a continuous flat surface. III. Boundary layer on a continuous cylindrical surface." AIChE J. **7**, 26-28. http://dx.doi.org/10.1002/aic.690070108

[16] Williamson, R.V. (1929). The flow of pseudoplastic materials. Ind. and Eng. Chem. **21**(11), 1108-1111. https://doi.org/10.1021/ie50239a035.